JOURNAL OF CATALYSIS **172,** 406–413 (1997)
ARTICLE NO. CA971798

Chlorine-Induced Restructuring of Ag(111) Films Observed by Scanning Tunneling Microscopy

Ernest R. Frank and Robert J. Hamers[1]

Department of Chemistry, University of Wisconsin–Madison, 1101 University Avenue, Madison, Wisconsin 53706

Received March 7, 1997; revised June 6, 1997; accepted June 18, 1997

The interaction of chlorine (Cl_2) with (111)-textured silver films has been studied using variable-temperature scanning tunneling microscopy. Real-time images reveal that Cl_2 adsorption produces a restructured surface consisting of large terraces separated by microfacets. This restructuring occurs at low chlorine exposures ($<5 \times 10^{-7}$ Torr · S), is observed with a variety of preparation conditions, and is thermally stable up to approximately 830 K. The observed restructuring may partially explain the role of chlorine on the selectivity enhancement observed in the epoxidation of ethylene catalyzed over silver catalysts.

It is well known that addition of trace amounts of impurities can greatly affect the selectivity and overall rates of heterogeneous catalytic reactions (1). Because these impurities are typically present in relatively small concentrations, identifying the mechanisms by which they affect surface chemical reactivity has been difficult. It is believed that these impurities affect reactivity and selectivity by modification of either the surface geometric and/or electronic structure. Studies on stepped surfaces and different crystal faces have, in some cases, shown that surface with high step densities are more active catalytically than low step density surfaces (2, 3) and are, therefore, believed to be the "active site." Atoms at steps have lower coordination than those in the bulk and, therefore, are likely to be more reactive. Additionally, the electron distribution at step edges is smoother than the distribution of positive charges; this electron-smoothing leads to a buildup of positive charge at the upper step edge and increased negative charge at the lower step edge (4). Recent scanning tunneling microscopy (STM) experiments have confirmed the preferential adsorption and rotational alignment of molecules at step edges of metal surfaces (5–9) as well as the preferential adsorption of xenon at step edges (10–13). While chemical reactions have yet to be observed at steps, the preferred adsorption and rotational alignment of molecules at steps show the importance steps play on the adsorption process.

Silver surfaces are widely used to catalyze the partial oxidation of organic compounds, particularly the epoxidation of ethylene (C_2H_4) to ethylene oxide (C_2H_4O) (1, 14–18). In the ethylene epoxidation reaction, chlorine added to the feed decreases the overall reaction rate but enhances the selectivity toward formation of the desired ethylene oxide product (19, 20). This selectivity enhancement has also been observed on studies performed over silver single crystals (16, 21–25), suggesting that single-crystal studies can provide insight that is relevant to the supported catalysts used in the industrial epoxidation reaction. In order to better understand the role of chlorine in modifying the selectivity and overall rate of the ethylene epoxidation reaction, we have used variable-temperature STM to investigate the interaction of chlorine with silver surfaces.

EXPERIMENTAL

Sample preparation and characterization were performed in a single ultrahigh vacuum system (base pressure 7×10^{-11} Torr) equipped with silver evaporators, Auger electron spectroscopy, low-energy electron diffraction (LEED), and a variable-temperature STM capable of operating between 110 and 450 K (26). Silver thin films were prepared by evaporation of approximately 5000 Å of silver onto a clean Si(111)-(7×7) surface heated to 850 K. *In situ* Auger electron spectroscopy shows that the evaporated films are pure silver free of impurities (<1%), while LEED shows sharp diffraction spots characteristic of a well-ordered (111) surface. STM images show that the surfaces prepared in this manner consist of flat atomic planes of (111) orientation which are several hundred angstroms wide, separated by monatomic steps. Fresh silver films were deposited for each experiment.

Surfaces characterized by LEED, Auger, and STM were exposed to Cl_2 through a variable leak valve. This was typically performed at a Cl_2 pressure of 2×10^{-9} Torr, although similar results were obtained at higher pressures. In some experiments, samples were exposed to Cl_2 at

[1] To whom correspondence should be addressed. E-mail: rjhamers@facstaff.wisc.edu.

0021-9517/97 $25.00

300 K while being imaged simultaneously with the STM; these experiments reveal the chlorine-induced structural changes in real time and allow one to discriminate between lateral variations in surface roughness, for example, and true adsorbate-induced restructuring events. To identify whether the chlorine-induced structural changes persisted at higher temperatures, experiments were also performed in which samples were exposed to Cl_2 while being heated to 520 K; these samples were subsequently imaged with STM after cooling to room temperature in vacuum.

RESULTS

Figure 1 shows three sequential STM images of a single 4000×4000 Å region of a freshly evaporated silver film as it is being exposed to Cl_2 at 300 K. Figure 1A shows the starting surface (before Cl_2 exposure) which consists of flat (111) terraces approximately 100 Å wide, separated by monatomic steps. In this particular image the steps are all oriented with outward normal along the $\langle 11\bar{2} \rangle$ direction, corresponding to a close-packed arrangement of atoms at the step edges. The region at the top left is highest with the surface stepping down to the right; this corresponds to an average miscut of approximately 1° from the (111) plane. Some step edges appear to be pinned locally, most likely by trace amounts of some unidentified impurity.

After the image in Fig. 1A was acquired, the leak valve was opened to begin introducing Cl_2 at a pressure of 2×10^{-9} Torr. Figure 1B shows the area *identical* to that shown in Fig. 1A. Since STM is a rastered technique and the surface was exposed to Cl_2 continuously during image acquisition, the Cl_2 exposure ranges from 0 L (1 L = 10^{-6} Torr · sec) at the top of Fig. 1B to 1.1 L at the bottom. The first thing to note is that at the top of Fig. 1B the steps appear more ragged than in Fig. 1A. Approximately half way through the acquisition of Fig. 1B, the STM image shows a rapid and dramatic surface restructuring. While the starting surface (Fig. 1A) consisted of relatively short Ag(111) terraces separated by monatomic steps, the Cl_2-exposed surface in the bottom portion of Fig. 1B consists of much larger terraces separated by large step arrays (microfacets). Figure 1C shows a third image of the same regions with a total Cl_2 exposure of approximately 3.0 L; here the surface restructuring appears to be complete. Images obtained after even higher exposures (not shown) show no further change, indicating that the surface modification is self-terminating after exposures of approximately 1 L. While Fig. 1B shows only a single sequence of images, repeated experiments on other samples show that the dramatic Cl-induced surface restructuring shown in Fig. 1 is a very reproducible phenomenon. Similar chlorine adsorption experiments performed at 110 K show the surface does not facet, but the atomic steps do roughen indicating preferential adsorption and reaction at step edges (27).

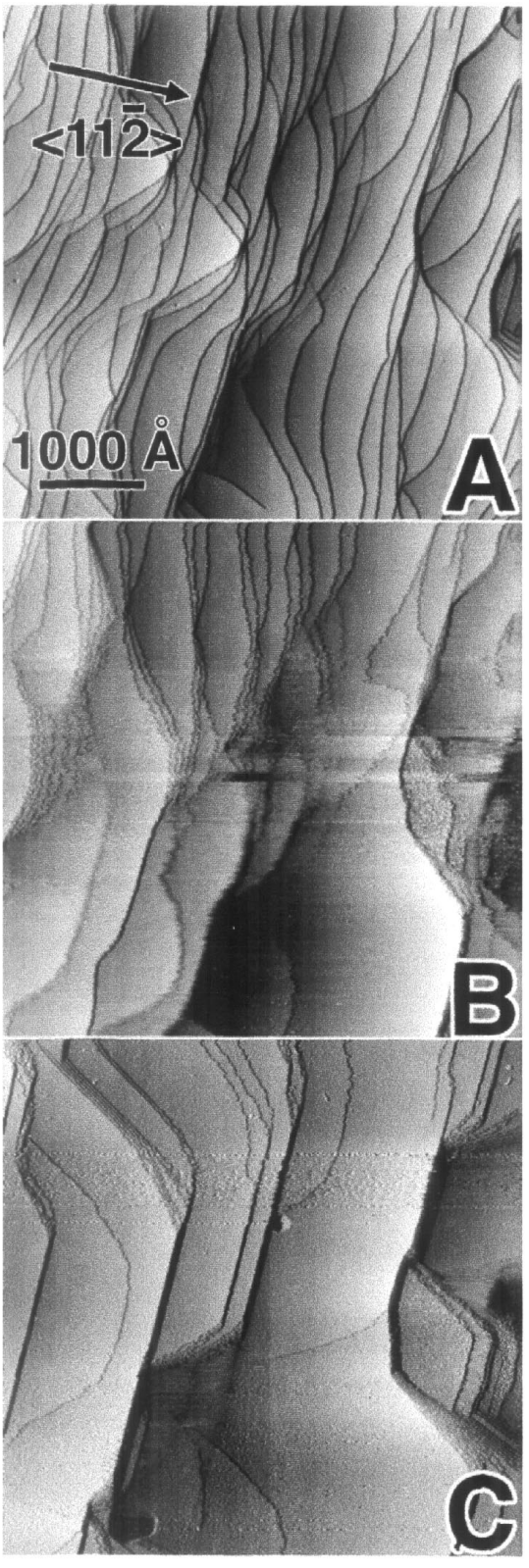

FIG. 1. Real-time monitoring of Cl_2 exposure on Ag(111) at room temperature. Dose started after (A). Time between images is 6 min. Steps are seen to initially roughen then bunch into two distinct periodicities. Dosing pressure, 2×10^{-9} Torr. Image size, 4000×4000 Å.

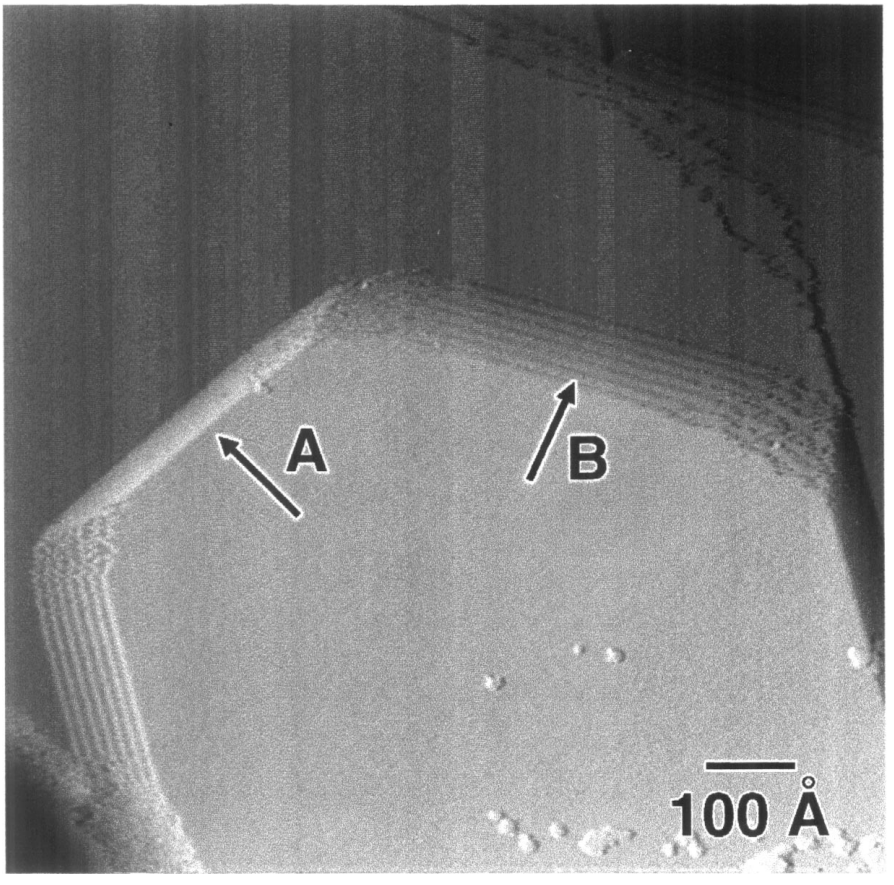

FIG. 2. Higher resolution image of the two step bunches. Steps running along the "A" direction have a separation of 6 lattice constants, while those running along the "B" direction have a separation of 15 lattice constants. Image size, 1000×1000 Å.

Because of the potential importance of steps in controlling the rate and selectivity of the ethylene epoxidation reaction, we obtained high resolution images of the Cl-induced microfacets. As shown in Fig. 2A, STM images reveal that the step arrays are formed at 60° angles with respect to one another. Closer inspection shows that there are two different types of step arrays, separated by 60°. Along the direction denoted "A" the steps are separated by 17.3 ± 1.5 Å, while along the "B" direction the step separation is 43.3 ± 2.3 Å. We attribute the presence of two different types of step arrays to the fact that although the topmost layer of the Ag(111) surface has hexagonal symmetry, the second layer reduces the overall rotational symmetry of the (111) plane to C_3. While these directions most likely correspond to steps close-packed steps with outward normal along the $\langle 11\bar{2} \rangle$ directions, because atomic resolution was not achieved it is not possible from the STM images alone to assign these directions unambiguously. Unfortunately, the possible errors in measurement of the horizontal distance between steps prevents assignment of a definitive crystallographic direction for the microfacets. Attempts to observe new diffraction spots from the microfacets using LEED were unsuccessful, apparently because the microfacets still constitute only a very small fraction of the total surface area and are also small, resulting in spots too weak and broad to observe.

To determine the amount of chlorine on the surface, Auger electron spectroscopy was performed on the chlorine-dosed Ag(111) films. The ratio of the Cl_{LMM} (181 eV) to Ag_{MNN} (351 eV) peak height for a film exposed at room temperature reaches a maximum at 0.41 in our experimental configuration. In Fig. 3 an Auger spectrum, acquired at the minimum Cl_2 exposure necessary to induce facetting, shows a Cl/Ag peak height ratio of 0.30. Although we are not able to determine the absolute Cl coverage, a previous study by Bowker and Waugh found that the saturation coverage of Cl on Ag was 0.52 monolayer (28); this would imply that in our experiments $\emptyset_{Cl} \leq 0.38$ monolayer for faceted surfaces such as those shown in Figs. 1 and 2. Because the microfacets account for only a small fraction of the total surface area, this result implies that most of the Cl must be adsorbed on the flat (111) terraces, with some possibly adsorbed at the facets.

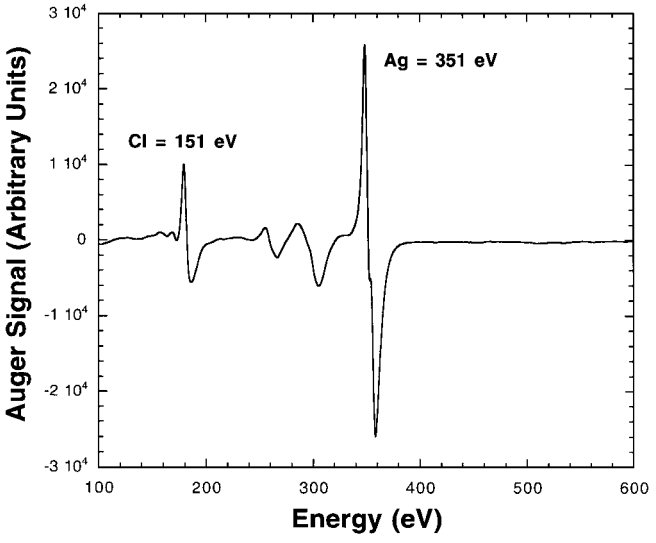

FIG. 3. Auger spectrum of the room temperature dosed Ag(111) film. Cl/Ag peak height ratio is 0.30. Total exposure 0.32 L. Saturation ($Ø_{Cl} = 0.52$) Cl/Ag height ratio is 0.41; absolute $Ø_{Cl} = 0.38$ for the facetted surface.

Attempts were made to identify where the Cl might be located using STM. At room temperature STM does not show any features that can be attributed to Cl atoms. However, similar experiments at low temperature (to be discussed elsewhere) (27) do show formation of an ordered overlayer. These results suggest that at room temperature the Cl atoms are simply too mobile to observe in STM.

Despite the fact that Cl atoms are mobile at 300 K, the microfacets appear to be quite stable over long periods of time. To determine the stability of the microfacetted surface at elevated temperatures comparable to those used in the ethylene epoxidation reactions, we performed two types of additional experiments. In some experiments samples were exposed to Cl_2 at room temperature and then annealed; in other experiments, Ag samples were exposed to Cl_2 at elevated temperatures. In both cases, STM experiments were performed after cooling the same back to room temperature. Both sets of experiments showed restructuring similar to that observed in Fig. 1B. In fact, the restructuring appears to be facilitated at elevated temperatures. The Cl-induced structural changes can be seen more quantitatively in Fig. 4. Figure 4 shows representative height profiles of a Ag(111) film immediately after dosing with Cl_2 at 300 K and the same surface after annealing to 520 K and then cooling back to 300 K for imaging. This graph shows a large change in the size of the microfacet (number of steps) and the average distance between the microfacets on the surface. While surfaces dosed at room temperature typically have terrace widths of several hundred angstroms between facets, chlorine exposed surfaces that have been annealed typically have terrace widths of several thousand angstroms. Thus, the Cl_2-induced restructuring is facilitated at elevated temperatures. To determine whether the Cl coverage is affected by annealing, we also measured Auger electron spectra before and after annealing Cl_2-exposed Ag films. Auger electron spectroscopy indicates a slight increase in Cl coverage. Typical samples yielded Cl/Ag Auger peak ratios of 0.41 ± 0.02 before annealing and 0.44 ± 0.02 after annealing to 520 K due to diffusion of subsurface chlorine to the surface (28). This is consistent with previous studies that have shown little or no desorption of Cl from the surface at this temperature (28, 29). More importantly, it demonstrates that the both the chemical composition and restructuring of the films persist at temperatures used in large-scale ethylene oxidation reactions.

The structures observed above are not strongly affected by sample temperature. At temperatures above approximately 670 K, however, previous studies have shown desorption of AgCl from Cl-exposed surfaces (28). After annealing to such high temperatures, our STM images show that the surface is characterized by roughened step edges and the appearance of "islands" on the large terraces; this can be seen in Fig. 5, which shows a Cl_2-exposed Ag(111) surface that was annealed to 830 K for 30 sec. Control experiments performed on perfectly clean Ag(111) films show a nearly identical behavior, suggesting that the formation of islands is not a result of Cl exposure but is due to a thermal roughening (30) of the Ag surface as the melting point is approached. Auger spectroscopy on this sample still shows the presence of some chlorine (Cl/Ag Auger peak ratio = 0.20), but in an amount significantly less than the original surface.

While the above experiments involved sequential dosing and annealing steps, we also conducted experiments in which Ag(111) films were exposed to chlorine gas while the sample was heated to 520 K, in order to more closely

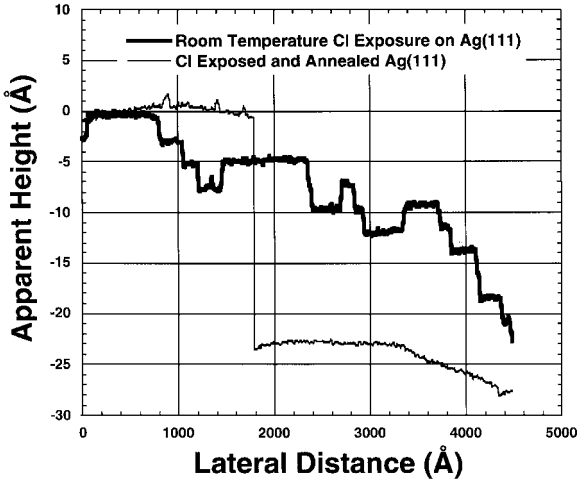

FIG. 4. Height profiles scans across an room temperature Cl exposed Ag(111) film and the same film annealed to 220°C. The height of and the spacing between the microfacets increases with annealing.

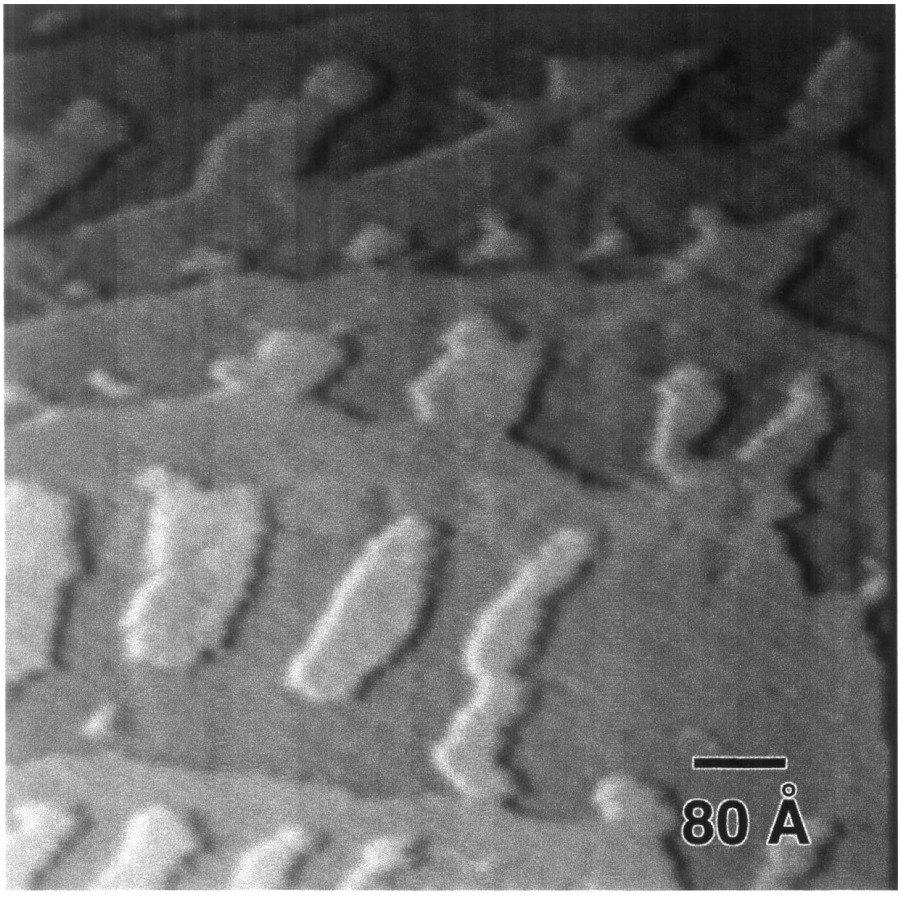

FIG. 5. STM image of a room temperature Cl dosed Ag(111) film annealed to 530°C. The reconstruction induced by Cl adsorption is lifted and the surface resembles a clean annealed Ag(111) film. Image size, 800 × 800 Å.

approximate conditions in industrial epoxidation reactions. The overall surface morphology was nearly identical to that of samples exposed to Cl_2 at room temperature and subsequently annealed, and Auger spectroscopy shows a similar Cl/Ag peak height ratio of 0.41 ± 0.04. More importantly, these preparation conditions are closest to the actual catalytic conditions where a feed gas containing chlorine or ethylene chloride is passed over a heated catalyst.

DISCUSSION

The above experimental results demonstrate that chlorine induces a microscopic scale restructuring of silver thin films in which short terraces and monatomic steps are replaced by much larger terraces and microfacets. Furthermore, this restructuring persists at temperatures that are widely used in the epoxidation of ethylene. This suggests the observed microfacets may play a role in the selectivity enhancement of chlorine in the catalytic epoxidation.

Despite a large number of studies devoted to understanding ethylene epoxidation, the mechanism of this reaction is still not completely understood. Chemisorbed atomic oxygen, chemisorbed molecular oxygen, and subsurface atomic oxygen are all observed on Ag surfaces (14). While studies have demonstrated that subsurface oxygen is necessary for the selective epoxidation (31), the role of the other forms of oxygen remain controversial. Studies performed by Kilty (32) on silver powders and kinetic studies performed on single crystals by Campbell *et al.* (16, 22, 23, 29, 33–35) have generally concluded that chemisorbed O_2 is responsible for epoxidation, while atomic oxygen is responsible for total oxidation to CO_2 and H_2O (16, 22, 34). However, isotopic labeling experiments suggest atomic oxygen is responsible for both epoxidation and combustion. A silver surface precoated with atomic ^{16}O and exposed to an $^{18}O_2/C_2H_4$ feed shows initial formation of $C_2H_4{}^{16}O$ as well as $C^{16}O_2$ and $H_2{}^{16}O$ (36). Likewise, silver surfaces exposed to an C_2H_4/N_2O feed, using N_2O as the oxygen source which decomposes on silver to N_2 and atomic oxygen, show both epoxidation and combustion of ethylene (37). Quantum chemistry calculations have suggested that reaction of oxygen with ethylene might take place via insertion of an electron-deficient (electrophilic) atomic oxygen into the C–H bond of ethylene (38–40) or via reaction of an

electron-rich atomic oxygen radical with the carbon–carbon π bond of ethylene.

Mechanistic models have suggested several possible roles for chlorine in enhancing ethylene epoxidation. Campbell and Koel (23, 29) and Carter and Goddard (41, 42) proposed that chlorine blocks specific surface sites at which total oxidation takes place; Campbell and Koel proposed specifically that total oxidation takes place at positivity-charge $Ag^{\delta+}$ surface sites. Others have proposed that enhanced selectivity can be attributed to high subsurface oxygen concentrations and that the role of chlorine is to roughen the surface, leading to enhanced subsurface oxygen and thereby to increased selectivity (43, 44). Electronic effects have also been proposed in which surface chlorine affects the ethylene oxide–surface bond in a way that inhibits isomerization to acetaldehyde (45) or substitutes subsurface oxygen and decreasing the electron density around chemisorbed atomic oxygen, thereby modifying its reactivity by creating an electron-deficient atomic oxygen species (38, 39).

Thus, the role of chlorine in enhancing epoxidation selectivity is complex and not yet resolved; indeed, more than one mechanism might be operative. Our observation of chlorine induced facetting of Ag(111) suggests possible routes for the effect of chlorine on the reactivity and selectivity of the catalytic epoxidation of ethylene. The creation of microfacets on the Ag(111) surface, with different step/terrace distribution, creates heterogeneous surface regions having distinct geometric and electronic structure and chemical reactivity. These local effects may play a role in the overall observed selectivity enhancement and are discussed below in the context of previously proposed models for the selectivity enhancement of chlorine on silver catalysts.

The most obvious way restructuring could affect reactivity is via a structural mechanism. If surface species are first adsorbed onto the surface and then diffuse to reactive sites, the probability of a diffusing surface species finding a step in a finite lifetime is greater on an unrestructured surface than on a restructured surface. This is shown in Fig. 6 which plots the probability a surface site is a given distance from an atomic step. On the undosed surface the average distance from a step is 97 Å; on the room temperature dosed surface the average distance to a step is 215 Å, and some molecules must diffuse more than 800 Å before encountering a step. Assuming that steps are sites favoring total oxidation because of the lower coordination number of step atoms and the perturbed electron distribution, one would then predict that the probability of an adsorbed ethylene molecule diffusing to an active site favoring and undergoing total oxidation would be less on a chlorine restructured surface than on an unrestructured surface. The overall effect would be a decrease in the total oxidation rate and an increase in selectivity toward epoxidation.

Although it is not known whether steps are the active sites for ethylene epoxidation, we note that at any step edge, the

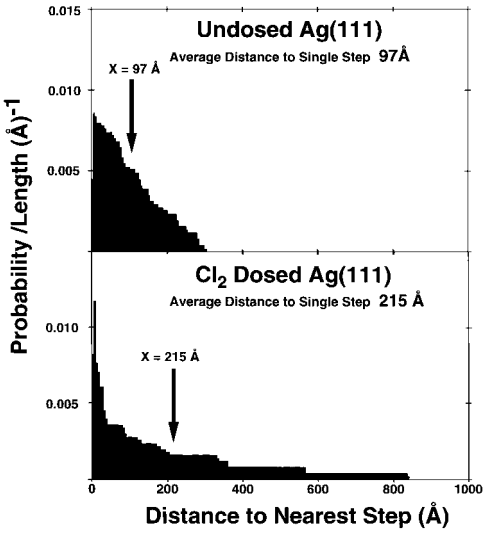

FIG. 6. Step distance probability distribution function for clean- and Cl-exposed Ag(111). The function represents the probability that a reactive molecule will diffuse a given distance before encountering a step. While the absolute number of steps remains constant, the spatial distribution of steps along the surface changes dramatically all surface sites being within 350 Å of a step edge in the undosed sample, while a significant number of surface sites are greater than 350 Å from steps on the chlorine dosed film.

spatial distribution of electrons is smoother than the distribution of nuclei. As a result, at a step edge the electrons spill over from the upper selvedge to the lower selvedge. This leaves the Ag atoms at the upper step edge positively charged and those at the lower edge negatively charged. Thus, silver atoms present at step edges might well be the partially charged $Ag^{\delta+}$ atoms proposed by Campbell and Koel as the site for total oxidation (23, 29). We note that under the conditions we have investigated, chlorine does not change the total number of steps or the number of step edge atoms; rather, by concentrating the steps into a smaller region, it increases the average distance that an impinging reactive molecule must diffuse in order to encounter a step edge. That is, the effect does not rely on the *number* of steps as much as on the *spatial distribution* of steps.

Because neither the residence time nor the diffusion coefficient of ethylene or oxygen on Ag(111) is known, it is not possible to determine the longest possible length which ethylene and/or oxygen could diffuse before reaching a reactive site or desorbing from the surface. However, our data can be analyzed to determine the probability distribution function for randomly impinging species finding a step edge after diffusing a given distance. Figure 6 shows such a normalized probability distribution; it shows that the average distance which an incident molecule must diffuse on the surface before encountering a step is 97 Å on the undosed surface and 215 Å on the Cl-exposed surface, an increase by a factor of 2.2. Although the overall reaction sequence

is still most likely complex, we note that if total oxidation takes place only at steps and partial oxidation takes place on the terraces, then one would expect that Cl would enhance the selectivity toward ethylene oxide by approximately a factor of 2.2. This is in qualitative agreement with previous studies that have shown that at an absolute coverage of $\emptyset_{Cl} = 0.4$ (a coverage at which we observe restructuring), the selectivity toward ethylene epoxidation on Ag(111) is increased by a factor of approximately 1.5 compared with that of a chlorine-free surface (29).

Another possible structural effect of chlorine would be to facilitate incorporation of subsurface oxygen. Subsurface oxygen arises from surface atomic oxygen diffusing into the bulk (31), and previous studies show that silver surfaces with adsorbed chlorine (25, 43) or roughened by ion bombardment (43, 44) have greater subsurface oxygen concentrations. The roughened surface provides necessary defect sites into which atomic oxygen can diffuse from the surface to the bulk (25, 31). Our studies show formation of microfacets which might allow more facile incorporation of oxygen into subsurface sites. Unfortunately, there exists no determination of incorporation of subsurface oxygen on different crystal faces of silver, in particular, comparison of rates of incorporation of low and high index crystal faces.

The microfacets present regions of distinct electronic structure as well as geometric structure. In general, highly stepped surfaces have lower work functions (46), resulting in more facile transfer of electrons out of the bulk. Previous studies on a number of surfaces have shown that oxygen adsorption proceeds through an O_2^- anion, and as a result the sticking coefficient of O_2 is much higher on stepped surfaces than on planar surfaces (47–49). Ethylene oxidation, however, requires dissociation of the adsorbed oxygen molecules to form atomic oxygen, and previous studies have shown that chlorine decreases the overall probability of *dissociative* adsorption (23, 25, 29, 32, 45). This at first appears to be in contradiction to our results. However, we note that these studies all measured the total oxygen concentration over the entire surface. Our results suggest that one might find strong local variations in the oxygen concentration.

Finally, the different electronic structure of the microfacets can also change the electronic structure of adsorbates bonded in the region. Quantum chemical calculations suggest that subsurface oxygen or chlorine affects the electronic character of surface oxygen (38–40). As mentioned previously, the smooth variations in electron density at step edges results in regions at upper step ledges with partial positive charge thus creating regions with an outer positive layer normal to the facet (4). Calculations suggest that an atomic oxygen stabilized by $Ag^{\delta+}$ surface sites creates an electrophilic oxygen species that inserts into the C–H bond of ethylene in the initial step (38, 39). While these previous authors proposed that the necessary $Ag^{\delta+}$ sites were formed by charge transfer to subsurface oxygen or subsurface chlorine, our results suggest that $Ag^{\delta+}$ atoms formed by electron smoothing at step edges and microfacets might also play an important role in the ethylene oxidation process.

Our results show that restructuring occurs only above a threshold of surface chlorine coverage (absolute $\emptyset_{Cl} \leq 0.38$). This in turn suggests that if restructuring is the dominant factor controlling the chlorine-induced selectivity enhancement, one would also expect very little improvement in selectivity at coverages below this value. While previous studies have shown the selectivity enhancement is approximately linear for absolute chlorine coverages up to approximately 0.26 on Ag(111) (22), it is likely that the overall kinetics are complicated and that our studies might not have investigated sufficiently large areas of the surface to determine accurately the dependence on $\emptyset_{Cl}$.

In conclusion, chlorine gas (Cl_2) adsorption on Ag(111) is shown to result in a dramatically restructured surface with very large terraces separated by microfacets. The restructured surface is stable up to 830 K and can be prepared under a variety of different conditions. Although there are several possible mechanisms by which chlorine might modify the reactivity, our direct observation of chlorines alteration of the surface sturcture on the atomic scale suggests that restructuring may be responsible in part for the observed selectivity enhancement of the ethylene epoxidation reaction.

ACKNOWLEDGMENTS

The authors acknowledge the National Science Foundation, the Union Carbide Corporation, and the Eastman Kodak Company for financial support.

REFERENCES

1. Madix, R. J., *in* "The Chemical Physics of Solid Surfaces and Heterogeneous Catalysis" (D. A. King and D. P. Woodruff, Eds.), p. 1. Elsevier, Amsterdam, 1982.
2. Somorjai, G. A., *Adv. Catal.* **26**, 1 (1977).
3. Somorjai, G. A., "Introduction to Surface Chemistry and Catalysis." Wiley, New York, 1994.
4. Smoluchowski, R., *Phys. Rev.* **60**, 661 (1941).
5. Frank, E. R., Chen, X., and Hamers, R. J., *Surf. Sci.* **334**, L709 (1995).
6. Chen, X., Frank, E. R., and Hamers, R. J., *Vacuum Sci. Technol. B* **14**, 1136 (1996).
7. Stranick, S. J., Kamna, M. M., and Weiss, P. S., *Science* **266**, 99 (1994).
8. Stranick, S. J., Kamna, M. M., and Weiss, P. S., *Surf. Sci.* **338**, 41 (1995).
9. Stroscio, J. A., and Eigler, D. M., *Science* **254**, 1319 (1991).
10. Weiss, P. S., and Eigler, D. M., *Phys. Rev. Lett.* **69**, 2240 (1992).
11. Zeppenfeld, P., Horch, S., and Comsa, G., *Phys. Rev. Lett.* **73**, 1259 (1994).
12. Land, T. A., Michely, T., Behm, R. J., Hemminger, J. C., and Comsa, G., *J. Chem. Phys.* **97**, 6774 (1992).
13. Horch, S., Zeppenfeld, P., and Comsa, G., *Appl. Phys. A* **60**, 147 (1995).
14. Barteau, M. A., and Madix, R. J., *in* "The Chemical Physics of Solid Surfaces and Heterogeneous Catalysis" (D. A. King and D. P. Woodruff, Eds.), p. 95. Elsevier, Amsterdam, 1982.
15. Sachtler, W. M. H., Backx, C., and Van Santen, R. A., *Catal. Rev. Sci. Eng.* **23**, 127 (1981).

16. Campbell, C. T., *in* "Catalyst Characterization Science Surface and Solid Stats Chemistry" (M. L. Deviney and J. L. Gland, Eds.), p. 210. Am. Chem. Soc., Washington, DC, 1985.
17. Verykios, X. E., Stein, F. P., and Coughlin, R. W., *Catal. Rev. Sci. Eng.* **22**, 197 (1980).
18. Van Santen, R. A., and Kuipers, H. P. C. E., *Adv. Catal.* **35**, 265 (1987).
19. Law, G. H., and Chitwood, H. C., "Process of Making Olefin Oxides." 1942.
20. Berty, J. M., *Chem. Eng. Commun.* **82**, 229 (1989).
21. Kummer, J. T., *J. Phys. Chem.* **60**, 666 (1956).
22. Campbell, C. T., *J. Catal.* **94**, 436 (1985).
23. Campbell, C. T., and Koel, B. E., *J. Catal.* **92**, 272 (1985).
24. Grant, R. B., and Lambert, R. M., *J. Catal.* **92**, 364 (1985).
25. Tan, S. A., Grant, R. B., and Lambert, R. M., *J. Catal.* **100**, 383 (1986).
26. Chen, X., Frank, E. R., and Hamers, R. J., *Rev. Sci. Instrum.* **65**, 3373 (1994).
27. Frank, E. R., and Hamers, R. J. [to be published]
28. Bowker, M., and Waugh, K. C., *Surf. Sci.* **134**, 639 (1983).
29. Campbell, C. T., *J. Catal.* **99**, 28 (1986).
30. Frenken, J. W. M., Hamers, R. J., and Demuth, J. E., *J. Vacuum Sci. Tech. A* **8**, 293 (1990).
31. Backx, C., Moolhuysen, J., Geenen, P., and Van Santen, R. A., *J. Catal.* **72**, 364 (1981).
32. Kilty, P. A., Rol, N. C., and Sachtler, W. M. H., *Int. Cong. Catal.* **2**, 929 (1972).
33. Campbell, C. T., *J. Vacuum Sci. Technol. A* **2**, 1024 (1984).
34. Campbell, C. T., and Paffett, M. T., *Surf. Sci.* **139**, 396 (1984).
35. Campbell, C. T., and Paffett, M. T., *Appl. Surf. Sci.* **19**, 28 (1984).
36. Van Santen, R. A., and Groot, C. P. M., *J. Catal.* **98**, 530 (1986).
37. Tan, S. A., Grant, R. B., and Lambert, R. M., *J. Catal.* **104**, 156 (1987).
38. Jorgensen, K. A., and Hoffmann, R., *J. Phys. Chem.* **94**, 3046 (1990).
39. van den Hoek, P. J., Baerends, E. J., and van Santen, R. A., *J. Phys. Chem.* **93**, 6469 (1989).
40. Van Santen, R. A., *Catal. Rev. Sci. Eng.* **37**, 557 (1995).
41. Carter, E. A., and Goddard, W. A., *J. Catal.* **112**, 80 (1988).
42. Carter, E. A., and Goddard, W. A., *Surf. Sci.* **209**, 243 (1989).
43. Wu, K., Wang, D., Wei, X., Cao, Y., and Guo, X., *J. Catal.* **140**, 370 (1993).
44. Wang, D., Wu, K., Cao, Y., Wei, X., and Guo, X., *Stud. Surf. Sci. Catal.* **75**, 1579 (1993).
45. Tan, S. A., Grant, R. B., and Lambert, R. M., *J. Catal.* **106**, 54 (1987).
46. Besocke, K., and Wagner, H., *Phys. Rev. B* **8**, 4597 (1973).
47. Hopster, H., Ibach, H., and Comsa, G., *J. Catal.* **46**, 37 (1977).
48. Ibach, H., Horn, K., Dorn, R., and Luth, H., *Surf. Sci.* **38**, 433 (1973).
49. Ibach, H., *Surf. Sci.* **53**, 444 (1975).